

LUMINESCENCE OF A NEW Ru(II) POLYPYRIDINE COMPLEX CONTROLLED BY A REDOX-RESPONSIVE PROTONABLE ANTHRA[1,10]PHENANTHROLINEQUINONEFrantišek HARTL^{a,*}, Sandrine VERNIER^b and Peter BELSER^{b1,*}^a Van't Hoff Institute for Molecular Sciences, Universiteit van Amsterdam, Nieuwe Achtergracht 166, 1018 WV Amsterdam, The Netherlands; e-mail: hartl@science.uva.nl^b Department of Chemistry, University of Fribourg, Chemin du Musée 9, 1700 Fribourg, Switzerland; e-mail: ¹ peter.belser@unifr.chReceived June 23, 2005
Accepted August 24, 2005

Redox-controlled luminescence quenching is presented for a new Ru(II)-bipyridine complex $[\text{Ru}(\text{bpy})_2(\mathbf{1})]^{2+}$ where ligand **1** is an anthra[1,10]phenanthrolinequinone. The complex emits from a short-lived metal-to-ligand charge transfer, ³MLCT state ($\tau = 5.5$ ns in deaerated acetonitrile) with a low luminescence quantum yield (5×10^{-4}). The emission intensity becomes significantly enhanced when the switchable anthraquinone unit is reduced to corresponding hydroquinone. On the contrary, chemical one-electron reduction of the anthraquinone moiety to semiquinone in aprotic tetrahydrofuran results in total quenching of the emission.

Keywords: Ruthenium; Polypyridine complexes; Anthraquinone; Phenanthrolines; Bipyridines; Electron transfer; Luminescence quenching; Electrochemistry; Redox switch; Cyclic voltammetry, UV-VIS spectroscopy.

Photoinduced energy- and electron-transfer processes in supramolecular systems with incorporated *p*-quinones are a topical area of growing interest. *p*-Quinones are important molecules in biological electron transport and can be utilised as regulators of electronic communication in electron-transfer systems based for example on porphyrins^{1,2}. Their easy functionalisation and well-defined reversible redox behaviour make them appealing candidates for construction of molecular electro-photoswitching devices³. Among the first studied inorganic systems belongs $[\text{Ru}(\text{bpy})_3]^{2+}$ with pendant 1,4-benzoquinone covalently linked through a flexible hydrocarbon chain to one of the 2,2'-bipyridine (bpy) ligands⁴. The luminescence of the metal complex is a function of the quinone redox state. Reversible interconversion between the 1,4-benzoquinone and hydroquinone forms of the two-electron redox couple was found to switch the luminescence off and

on, respectively. A similar efficient quenching effect was observed for electrogenerated chemiluminescence of $[\text{Ru}(\text{bpy})_3]^{2+}$ in the presence of 1,4-benzoquinones, hydroquinones, phenols and catechols⁵. A series of chromophore-quencher dyads based on a 9,10-anthraquinone acceptor were studied by Meyer et al.⁶ More advanced is a donor-acceptor triad with the 1,4-benzoquinone/hydroquinone redox couple linking the luminescent $[\text{Ru}(\text{bpy})_3]^{2+}$ unit with a secondary $[\text{Co}(\text{bpy})_3]^{3+}$ electron acceptor⁷. More recently, a hydroquinone-functionalised 2,2':6',2''-terpyridine (tpy) ligand coordinated to an ethynylated Ru(II)-tpy fragment was studied as a chromophore-quencher dyad, with the hydroquinone/benzoquinone on/off level of the switch being temperature-dependent⁷.

In this paper we present a new electron donor-acceptor dyad based on a light-absorbing $\{\text{Ru}(\text{bpy})_2\}^{2+}$ unit complexed to a 1,10-phenanthroline-type (phen) ligand with fused 9,10-anthraquinone moiety (compound **1** in Chart 1). The advantage of this rigid π -system is a fixed metal-quinone distance that will facilitate a more rigorous description of the photophysical behaviour of the dyad⁸. The main goal of the present study was to understand the redox behaviour of the anthraquinone centre in $[\text{Ru}(\text{bpy})_2(\mathbf{1})]^{2+}$ (**2**) and to test its influence on the luminescence properties of the Ru(II)-polypyridine chromophore. The experimental results are compared with the literature data⁹ obtained for a series of structurally related reference complexes $[\text{Ru}(\text{bpy})_2(\text{L}')^{2+}$, with $\text{L}' = \text{np}$, dppz , dcnp , pd depicted in Chart 1, and bpy .

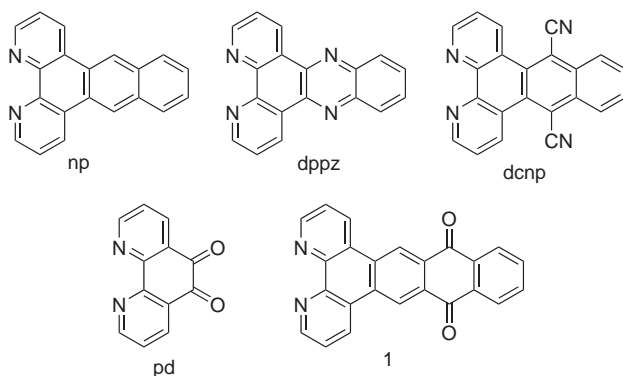
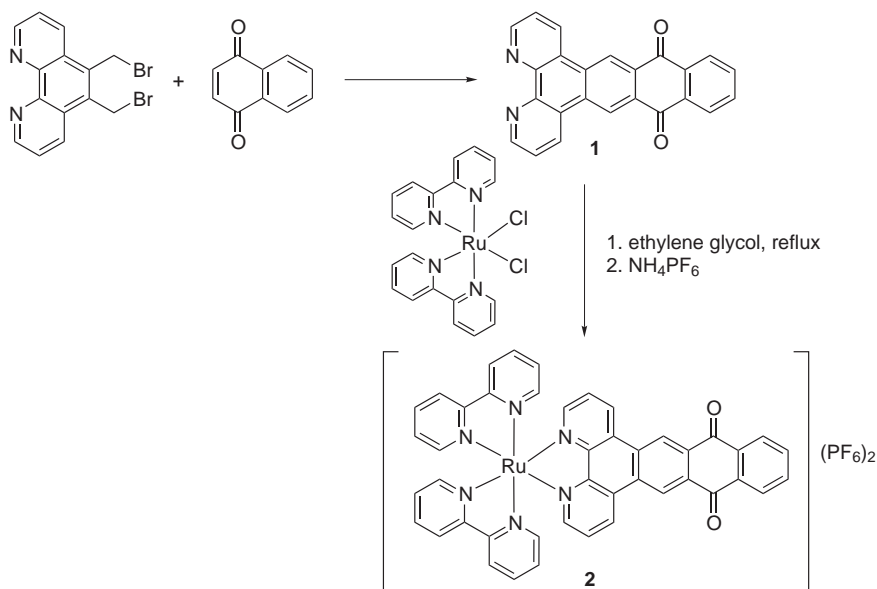


CHART 1

RESULTS AND DISCUSSION

Syntheses of Ligand 1 and Complex 2

Ligand **1** was prepared by Diels–Alder cycloaddition of 5,6-bis(bromo-methyl)-1,10-phenanthroline and 1,4-naphthoquinone (Scheme 1). The merely moderate yield is probably caused by the retro Diels–Alder reaction. The photochemical radical bromination of the methyl groups in the 5,6-dimethyl-1,10-phenanthroline precursor using *N*-bromosuccinimide facilitates the direct closure of the aromatic ring without using an oxidising agent¹⁰. Complex **2** was then obtained by heating poorly soluble crude ligand **1** with 1 equivalent of $[\text{RuCl}_2(\text{bpy})_2]$ in ethylene glycol for 2 h.



SCHEME 1

Redox Behaviour of Ligand 1 and Complex 2

Cyclic and Differential Pulse Voltammetry

Voltammetric studies of ligand **1** and complex **2** were performed with the aim to provide a good initial guess of the localisation of the individual redox processes in the complex and the nature of its frontier orbitals. These results are of fundamental importance for the discussion of the electronic

absorption and luminescence properties of complex **2**. The series of investigated compounds was completed with 9,10-anthraquinone as a suitable model for the acceptor moiety in ligand **1**. The electrode potentials and the localisation of the redox processes are given in Table I. The assignment of the redox active centres has been facilitated by comparison with literature electrochemical data for selected Ru(II) complexes closely related to complex **2**.

Anthraquinone. The cyclic voltammogram of anthraquinone in acetonitrile shows fully reversible reduction to the corresponding semiquinone radical anion at $E_{1/2} = -1.36$ V vs Fc/Fc⁺. The second cathodic step at $E_{1/2} = -2.02$ V producing the dianion is electrochemically quasireversible ($\Delta E_p = 120$ vs 80 mV for Fc/Fc⁺) but no coupled chemical reaction (protonation) was observed on the sub-second time scale ($I_{p,a}/I_{p,c} = 1$ at $v = 100$ mV s⁻¹). A very similar result was obtained in *N,N*-dimethylformamide¹².

Ligand 1. The redox behaviour of ligand **1** is very close to that of anthraquinone. The electrode potentials of the two cathodic steps localised on the *p*-quinone moiety are slightly shifted to less negative values (Table I). The quasireversible nature of the second cathodic step is maintained ($\Delta E_p = 90$ vs 70 mV for Fc/Fc⁺). The reduction of the non-coordinating phenan-

TABLE I
Electrochemical data for ligand **1**, complex **2** and reference compounds^a

Compound	Ru ^{II/III}	L ^{0/-1}	L ^{-1/-2}	bpy ^{0/-1} (1)	bpy ^{0/-1} (2)	phen ^{0/-1}
9,10-Anthraquinone ^b		-1.36	-2.02			
pd ^c		-0.85	-1.65			
1		-1.31	-1.88			
2	0.91	-1.19	-1.73	-1.81	-2.02	-2.43
2 ^d		-1.23	-1.75	-1.81	-2.02	-2.49
[Ru(bpy) ₂ (<i>N,N'</i> -pd)] ^{2+ c}	0.95	-0.56	-1.29			
[Ru(bpy) ₂ (dcnp)] ^{2+ e}	0.85	-1.15		-1.70	-1.90	-2.07
[Ru(bpy) ₂ (np)] ^{2+ e}	0.84			-1.78	-1.95	
[Ru(bpy) ₂ (dppz)] ^{2+ e}	0.84	-1.42		-1.84	-2.07	
[Ru(bpy) ₃] ^{2+ e}	0.89			-1.72	-1.93	

^a Conditions: acetonitrile (unless stated otherwise), 293 K, potentials vs Fc/Fc⁺. For comparison with literature data^{9a,11}, $E_{1/2}$ (Fc/Fc⁺) = 0.40 V vs SCE (acetonitrile). In the complexes, L denotes the aromatic acceptor moiety in the composed 1,10-phenanthroline (phen)-type ligands depicted in Chart 1. ^b This work. ^c Ref.¹¹ ^d In THF. ^e Ref.^{9a}

throline moiety was not observed in the available negative potential window of the acetonitrile electrolyte.

Complex 2. The cyclic voltammogram of complex **2** in acetonitrile shows a one-electron oxidation of the Ru(II) centre at $E_{1/2} = 0.91$ V vs Fc/Fc⁺, which is slightly more positive compared to the reference complexes in Table I. This small shift may reflect the presence of the acceptor anthraquinone component of ligand **1**. The first cathodic wave of complex **2** at $E_{1/2} = -1.19$ V is assigned to one-electron reduction of ligand **1** largely localised at the anthraquinone site. Compared to free anthraquinone and **1**, this cathodic step occurs less negatively, which is explained by stabilisation of the quinone π -system due to coordination of ligand **1** through the phenanthroline chelate. This result reveals an interaction between the fused phenanthroline and anthraquinone redox centres of ligand **1** that are not fully independent. The other cathodic waves of complex **2** in acetonitrile were strongly affected by adsorption at the electrode surface and acceptable resolution could only be achieved at a low concentration ($\sim 10^{-4}$ mol l⁻¹), using the differential pulse voltammetry technique (Table I). The cathodic part of the cyclic voltammogram of complex **2** was therefore recorded in THF (Table I and Fig. 1). The cyclic voltammogram shows the well separated initial reduction of the anthraquinone moiety to anthrasemiquinone, followed by two greatly overlapping cathodic steps. Considering only the values of the electrode potentials (Table I), obtained with a higher accuracy

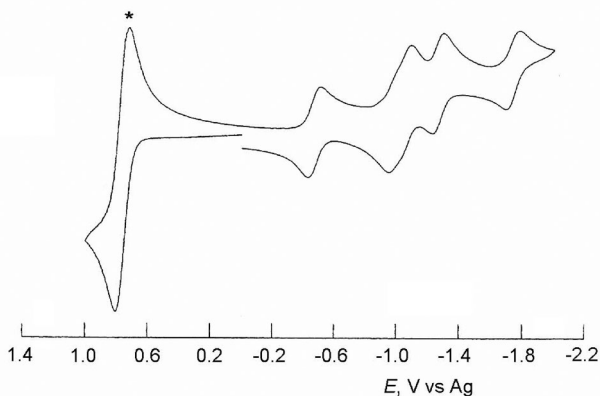


FIG. 1
Cyclic voltammogram of complex **2** recorded in THF at 293 K. The asterisk denotes the reference ferrocene/ferrocenium couple. Conditions: Pt disk electrode, $\nu = 100$ mV s⁻¹

from the corresponding differential pulse voltammogram (Fig. 2), it is difficult to decide whether the second cathodic step $E_{1/2} = -1.73$ V is localised on the ancillary 2,2'-bipyridine ligands or whether the anthrasemiquinone site in 2^- reduces first. The answer was sought in a UV-VIS spectroelectrochemical experiment (see below). The fourth reduction at $E_{1/2} = -2.02$ V involves the second 2,2'-bipyridine ligand, as revealed by the comparison with the reference complexes (Table I). The fifth cathodic step then occurs with a high probability at the coordinating phenanthroline redox centre of ligand 1^{2-} . It lies more negatively than the initial reductions of the 2,2'-bipyridine ligand, mainly as the consequence of the preceding two-electron reduction of the anthraquinone moiety. The voltammetric response of complex **2** does not provide any evidence for protonation of reduced ligand 1^{n-} ($n = 1-3$), all cathodic steps being fully reversible in the sub-second time domain.

UV-VIS Spectroelectrochemistry

Anthraquinone. One-electron reduction of the acceptor building block of ligand **1** produces the stable semiquinone radical anion. Its UV-VIS spectrum in acetonitrile at 293 K (Fig. 3) shows two structured absorption bands centred at 400 and 550 nm. The third, very broad, structured band lies in the near infrared region, below 700 nm. All these absorption features are due to intraligand (IL) electronic transitions involving the singly occupied

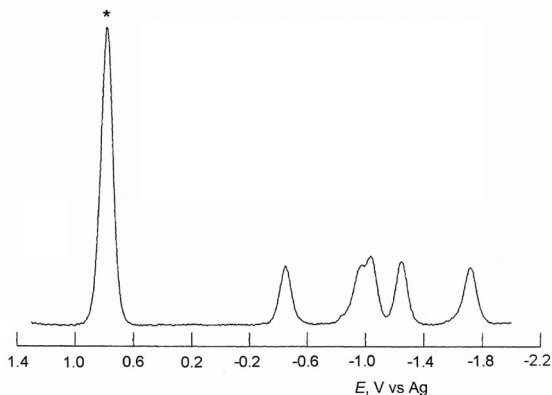


FIG. 2

Differential pulse voltammogram of complex **2** recorded in THF at 293 K. The asterisk denotes the reference ferrocene/ferrocenium peak. Conditions: Pt disk electrode, $\nu = 20$ mV s⁻¹, step increment 3 mV. The same sample as shown in Fig. 1

π^* orbital. Further reduction leads to disappearance of the near infrared band. The band at 400 nm further grows and changes its shape, while the band at 550 nm develops to a broad unresolved band centred at 520 nm (Fig. 4). Reverse oxidation of the two-electron reduction product is shifted to a less negative potential by ca. 1 V, as confirmed by the thin-layer cyclic voltammogram recorded along with the UV-VIS spectral changes, and results directly in the full recovery of parent anthraquinone. Such behaviour

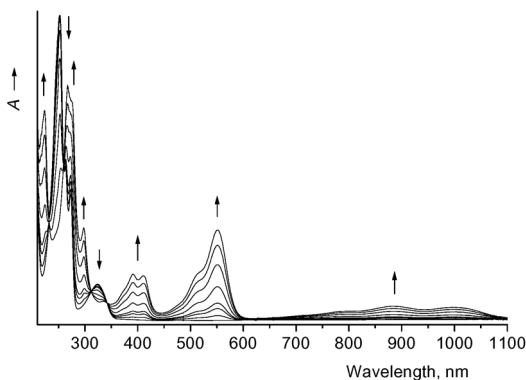


FIG. 3

UV-VIS spectral changes accompanying one-electron reduction of anthraquinone to anthraquinone radical anion. Conditions: butyronitrile, 293 K, OTTLE cell

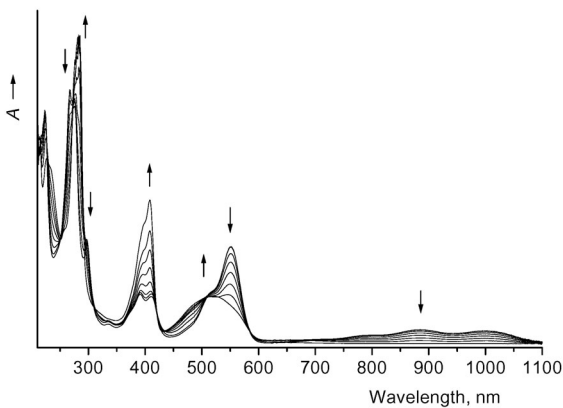


FIG. 4

UV-VIS spectral changes accompanying one-electron reduction of anthraquinone radical anion to anthrahydroquinone. Conditions: butyronitrile, 293 K, OTTLE cell

is characteristic of protonation of the anthraquinone-based dianion to anthrahydroquinone¹². Figures 3 and 4 serve as an important diagnostic tool for the discussion of the cathodic responses of ligand **1** and complex **2**.

Ligand 1. The UV-VIS spectrum of ligand **1** differs from that of anthraquinone in the presence of a weak absorption band centred at 595 nm, which gives ligand **1** its purple colour in solution (solid **1** is greenish gray). As this band is absent in the UV-VIS spectrum of complex **2** (see below), it may belong to an electronic transition involving the lone pairs at the non-coordinated phenanthroline nitrogens and directed toward the adjacent π -acceptor anthraquinone subunit. The $\pi\pi^*$ band of the quinone moiety is red-shifted to 380 nm compared to free anthraquinone (325 nm).

One-electron reduction of ligand **1** is accompanied by similar spectral changes as observed in the case of anthraquinone. In the visible region, a structured band appears at 440 nm, which has an equivalent in the 400 nm band of anthrasemiquinone. The 550 nm IL band of anthrasemiquinone is also shifted to lower energies (720 nm) in 1^- ; the equivalent of the broad and weak NIR absorption below 700 nm was not observed down to 1000 nm (Fig. 5). The second one-electron cathodic step then produced again the protonated anthrahydroquinone form of 1^{2-} (H_21), as confirmed by the appearance of the absorption band at 515 nm with a shoulder tailing to 800 nm (Fig. 5). The long-wavelength shoulder may belong to a π - π^* transition involving the anthrahydroquinone and phenanthroline subunits of H_21 (ref.¹³). Another characteristic feature in the absorption spectra of 1^-

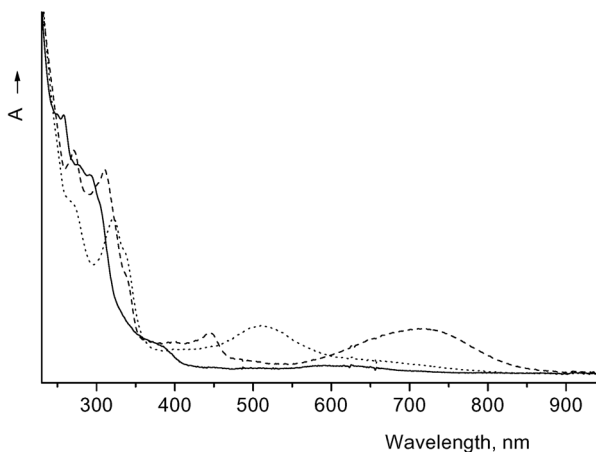


FIG. 5

UV-VIS spectra of ligand **1** (full line), 1^- (dashed line) and protonated 1^{2-} with anthrahydroquinone moiety (H_21 ; dotted line). Conditions: butyronitrile, 293 K, OTTLE cell

and H_21 is the fairly intense UV band (with a shoulder) at 315 and 320 nm, respectively, which lies above 300 nm in the case of anthrahydroquinone.

Complex 2. According to the electrochemical data in Table I, the one-electron reduction of complex **2** also largely resides on the anthraquinone moiety. This assignment is strongly supported by the appearance of the low-energy IL absorption band of 2^- (in THF) at 900 nm (Fig. 6), which is further red-shifted compared to the corresponding absorption of 1^- (Fig. 5), in agreement with the less negative reduction potential of complex **2**. The equivalent of the 440 nm band of 1^- is found in the absorption spectrum of 2^- at 470 nm; however, in this case, the Ru-to-bpy MLCT absorption also lies in this region (see below). The singly reduced 2,2'-bipyridine ligand, free¹⁴ or, for example, in $[Ru(bpy)_3]^n$ ($n = +1, 0$) (ref.¹⁵) or $[Cr(bpy)(CO)_4]^-$ (ref.¹⁶) absorbs strongly between 500–600 nm but its $\pi^*\pi^*$ IL absorption below 700 nm has a much lower intensity.

The second one-electron reduction of complex **2** at -1.75 V was studied carefully in the OTTLE cell using small negative potential steps in order to distinguish it from the partly overlapping third cathodic step (Figs 1 and 2, Table I). The result is depicted in Fig. 7. Clearly, the observed spectral changes in the visible spectral region nicely correspond with the absorption spectrum of protonated H_21 (Fig. 5). Hence, the protonation of the doubly reduced anthraquinone moiety takes place also in the doubly reduced complex, 2^{2-} , although this process is not observable by cyclic voltammetry on the sub-second time scale.

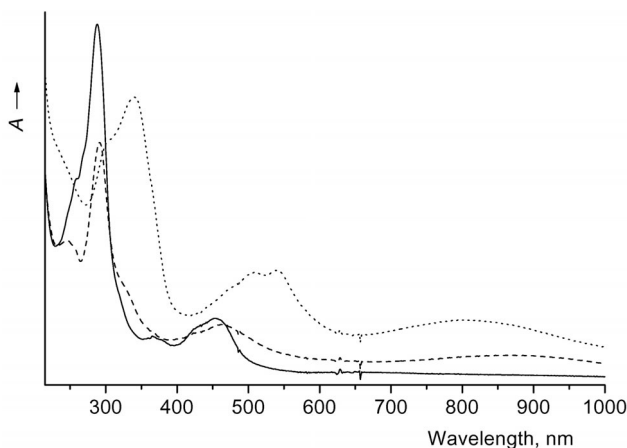


FIG. 6

UV-VIS spectra of complex **2** (full line), 2^- (dashed line) and the three-electron reduction product (dotted line). Conditions: THF, 293 K, OTTLE cell

The onset of the poorly separated third cathodic step at -1.81 V is indicated by a structured absorption band at 530 nm. This diagnostically important band is also observed in the UV-VIS spectrum of the one-electron-reduced complex $[\text{Ru}(\text{bpy})_3]^+$ (ref.¹⁵); it belongs to the red-shifted Ru-to-bpy CT band overlapping with an IL absorption of the radical anion of 2,2'-bipyridine. We can therefore safely conclude that the first two cathodic steps of complex **2** are localised at the anthraquinone subunit of ligand **1** and only the third and fourth one-electron reductions occur at the 2,2'-bipyridine ligands, after double protonation of $\mathbf{1}^{2-}$. In this regard, complex **2** differs from $[\text{Ru}(\text{bpy})_2(\text{dcnp})]^{2+}$ containing the comparably strong acceptor ligand dcnp (Chart 1 and Table I) that is only singly reduced prior to the following cathodic steps localised at the 2,2'-bipyridine ligands^{9a}.

The voltammetric and spectroelectrochemical measurements strongly support a substantial electronic separation between the fused phenanthroline and acceptor anthraquinone components of ligand **1**. The facile formation of the anthrahydroquinone system by the consecutive two-electron reduction of free anthraquinone occurs also in ligand **1** and complex **2**, as documented by UV-VIS spectroscopy. The stepwise two-electron reduction of ligand **1** in complex **2** does not significantly destabilise the lowest unoccupied $\pi^*(\text{bpy})$ orbitals, which causes a partial overlap of the anthrasemiquinone- and bpy-based cathodic waves. This would not be the case if the phenanthroline π -system of ligand **1** were substantially involved in the initial cathodic steps, increasing electronic repulsion between re-

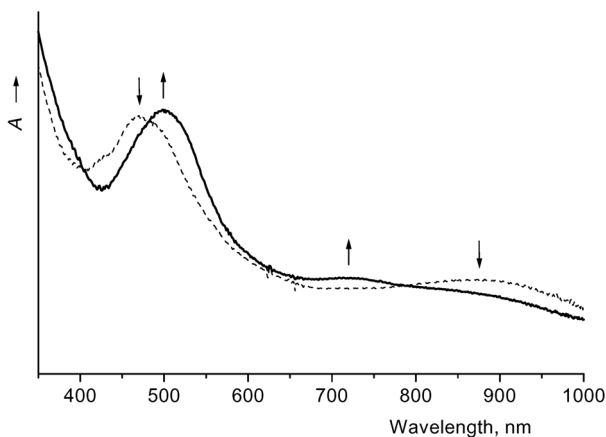


FIG. 7

UV-VIS spectral changes accompanying one-electron reduction of $\mathbf{2}^-$. Conditions: THF, 293 K, OTTL cell

duced ligand **1** and the ancillary 2,2'-bipyridine ligand and, hence, separation of the second and third cathodic waves. On the other hand, the electronic communication between the fused anthraquinone and phenanthroline units is not completely negligible, as indicated by a new electronic transition of ligand **1** at 595 nm (Fig. 5) and by stabilisation (~0.1 eV) of the quinone redox orbital upon coordination of ligand **1**. For comparison, this stabilisation is much larger (~0.3 eV) for the condensed 1,10-phenanthroline-5,6-dione (pd) ligand (Chart 1 and Table I).

Electronic Absorption and Luminescence of Complex **2**

The UV-VIS spectrum of complex **2** (Fig. 6) closely resembles that of $[\text{Ru}(\text{bpy})_3]^{2+}$, showing the strong $\pi\pi^*(\text{bpy})$ band at 285 nm and the composed Ru-to-bpy CT band centred at 450 nm. The CT transition to the phenanthroline part of chelated ligand **1** probably also falls within this absorption. The molar absorption coefficient of the MLCT band of complex **2** is higher compared to $[\text{Ru}(\text{bpy})_3]^{2+}$ and other reference complexes^{9a} in Table II. The new band at 365 nm can be attributed to a $\pi-\pi^*$ transition within the anthraquinone moiety (cf. Fig. 3). Another anthraquinone-centred absorption can be traced between 240–270 nm. There is no spectroscopic evidence for a CT transition from the Ru(II) centre to the acceptor anthraquinone moiety.

TABLE II

Electronic absorption spectra and emission data of complex **2** and selected reference^{9a} compounds^a

Complex		$\lambda_{\text{abs}}, \text{ nm}$ ($\epsilon_{\text{max}}, \text{ l mol}^{-1} \text{ cm}^{-1}$)	$\lambda_{\text{em}}, \text{ nm}$	$\tau, \text{ ns}$	$\Phi_{\text{em}} \times 10^{-3}$
2	deaerated	451 (18300)	610	5.5	0.5
$[\text{Ru}(\text{bpy})_2(\text{dcnp})]^{2+}$	aerated	439 (14600)	700	120	0.5
	deaerated		610 ^b	1700, 185	2
$[\text{Ru}(\text{bpy})_2(\text{np})]^{2+}$	aerated	452 (15100)	610	170	16
	deaerated		610	834	82
$[\text{Ru}(\text{bpy})_2(\text{dppz})]^{2+}$	aerated	448 (15700)	667	229	390
	deaerated		610	260	
$[\text{Ru}(\text{bpy})_3]^{2+}$	aerated	450 (13000)	611	190	12
	deaerated		611	1000	60

^a Conditions: acetonitrile, 298 K. ^b Emission maximum of a multicomponent band.

The difference transient absorption spectrum of complex **2** in deaerated acetonitrile was recorded in the nanosecond time domain upon excitation at 450 nm (Fig. 8). It shows the bleached MLCT band at 450 nm which decays mono-exponentially with a lifetime of 4.5 ns to restore the pre-pulsed baseline. The transient absorption between 500–820 nm probably belongs to a charge-transfer excited state with a negative charge on ancillary 2,2'-bipyridine ligands and/or (given the bandwidth) on the extended π -system of the 1,10-phenanthroline subunit of ligand **1**. The anthrasemiquinone absorption in a charge-separated excited state can be excluded, since the MLCT bleach would otherwise be less developed and differently shaped, and there would be no strong transient absorption starting already at 400 nm (see Fig. 6). The MLCT assignment is also supported by the photophysical properties of complex **2** (see below).

The emission spectrum of complex **2** was recorded in acetonitrile at 293 K (Fig. 9). The photophysical data and comparison with the reference compounds are presented in Table II. The luminescence of **2** is observed in deaerated acetonitrile at 610 nm, similarly to the emission maximum of $[\text{Ru}(\text{bpy})_3]^{2+}$. However, compared to the reference complex, the emission is very weak ($\Phi_{\text{em}} = 5 \times 10^{-4}$) and decays with a much shorter lifetime (5.5 ns), which is close to the 4.5 ns value measured for the transient in the nanosecond TA spectra (Fig. 8). In air-equilibrated acetonitrile, the emission intensity of complex **2** further drops. This behaviour agrees with population

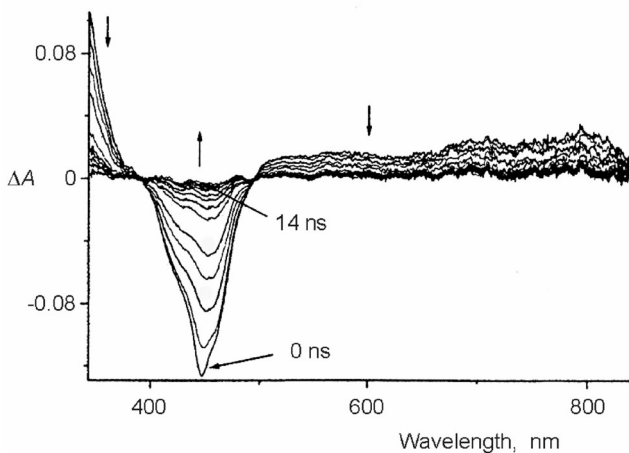


FIG. 8

Difference transient absorption spectra of complex **2** in deaerated acetonitrile solution ($\lambda_{\text{exc}} = 450$ nm, 2 ns FWHM, 1 ns increment time delay)

of the emitting Ru-to-bpy and/or Ru-to-phen $^3\text{MLCT}$ excited states. The fast decay and very low emission quantum yield point to efficient quenching of the $^3\text{MLCT}$ emission by electron transfer to the acceptor anthraquinone moiety of ligand **1** and rapid recovery of the ground state by charge recombination^{6,8}. By contrast, energy transfer occurs in the $^3\text{MLCT}$ excited state of the complex $[\text{Ru}(\text{bpy})_2(\text{dcbp})]^{2+}$ to the extended π -system of the anthracenedicarbonitrile moiety, resulting in a two weakly emitting charge transfer excited states (Table II)^{9a}. At low temperatures, and also in the other reference complexes $[\text{Ru}(\text{bpy})_2(\text{dppz})]^{2+}$ and $[\text{Ru}(\text{bpy})_2(\text{np})]^{2+}$, the $^3\text{MLCT}$ state is in a (solvent-dependent) thermal equilibrium with a slightly lower-lying ^3IL state of the acceptor subunit, which further increases the emission lifetime and intensity compared to $[\text{Ru}(\text{bpy})_3]^{2+}$ (ref.^{9a}). We have no evidence for such energy transfer to the anthraquinone moiety in complex **2**.

Chemical Reduction of Ligand **1** and Luminescence of Complex **2**

Complex **2** was reacted with cobaltocene and $\text{Na}_2\text{S}_2\text{O}_4$ in order to prove whether its weak emission is affected by chemical reduction of the anthraquinone site.

According to data in Table I, cobaltocene ($E_{1/2} = -1.34$ V vs Fc/Fc^+) is capable of reducing complex **2** exclusively to $\mathbf{2}^-$. Addition of cobaltocene (1 equivalent or in excess) to a solution of complex **2** in dry acetonitrile led to complete disappearance of the emission band observed for non-reduced

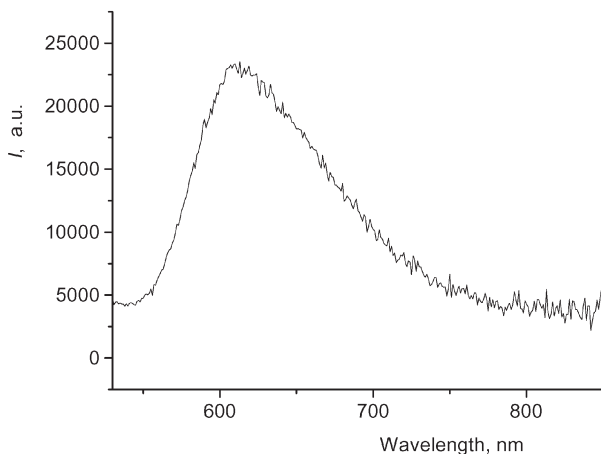


FIG. 9
Emission spectrum of complex **2** in deaerated acetonitrile ($\lambda_{\text{exc}} = 450$ nm, $A = 0.1$, $l = 1$ cm)

2 at 610 nm. This result can be ascribed⁸ to quenching of the $\text{*Ru}^{\text{III}}(\text{bpy}^{\cdot-})$ and/or $\text{*Ru}^{\text{III}}(\text{phen}^{\cdot-})$ charge transfer excited states by electron transfer from the reduced anthrasemiquinone moiety to Ru(III). This process is reversible and the emission of complex **2** could be restored by addition of an excess of FcBF_4 .

In contrast to the reduction with cobaltocene, addition of 2 equivalents of $\text{Na}_2\text{S}_2\text{O}_4$ in a small amount of water to a solution of complex **2** in acetonitrile led to a substantial increase in the emission intensity (Fig. 10). The UV-VIS absorption spectrum of the resulting orange solution showed new features at 330 nm and around 450–500 nm, but no absorption below 750 nm, which is consistent with the formation of the doubly protonated form of 2^{2-} containing the anthrahydroquinone¹² moiety (Figs 5 and 7). For comparison, addition of the same amount of water containing no reducing agent caused much less pronounced enhancement of the luminescence intensity (Fig. 10). Apparently, the anthrahydroquinone moiety does not act as a quencher and the emitting excited state becomes longer-lived, resulting in improved luminescence properties.

Further reduction with more than 2 equivalents of $\text{Na}_2\text{S}_2\text{O}_4$, which is localised at the ancillary 2,2'-bipyridine ligands, led again to diminished luminescence, similar to the quenching of emission by electron transfer caused by the one-electron reduction of the anthraquinone moiety in **2** with cobaltocene.

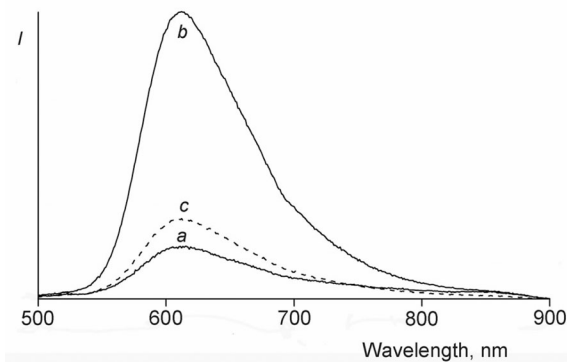


FIG. 10

Steady-state emission spectra of 4.1×10^{-5} M **2** *a* in deaerated dry acetonitrile (4 ml), *b* after addition of 2 equivalents of $\text{Na}_2\text{S}_2\text{O}_4$ in water (20 μl) and *c* after addition of water (20 μl) ($\lambda_{\text{exc}} = 450$ nm, $A = 0.74$, $l = 1$ cm)

Conclusions

The Ru-to-bpy and/or Ru-to-phen photoexcitation of complex **2** in acetonitrile results in the population of a relatively short-lived and weakly emitting $^3\text{MLCT}$ state compared to the photophysical properties of the reference complex $[\text{Ru}(\text{bpy})_3]^{2+}$. There is no evidence for an equilibrium between the $^3\text{MLCT}$ state and a ^3IL state localised on the anthraquinone moiety in ligand **1**, in difference from the situation encountered^{9a} in the other reference complexes $[\text{Ru}(\text{bpy})_2(\text{L}')^{2+}$ ($\text{L}' = \text{dppz}, \text{np}, \text{dcnp}$; see Chart 1). The luminescence quenching is probably caused by intramolecular electron transfer in the $^3\text{MLCT}$ state to the adjacent anthraquinone receptor and concomitant charge recombination. Similarly to the light-induced reduction of the anthraquinone moiety, one-electron chemical reduction producing the anthrasemiquinone donor results in fully quenched emission due to electron transfer to the photoexcited $\{^*\text{Ru}^{\text{III}}(\text{bpy}^{\cdot-})\}$ and/or $\{^*\text{Ru}^{\text{III}}(\text{phen}^{\cdot-})\}$ luminophores. The reductive quenching is switched off by protonation of the anthraquinone-dianion moiety in $\mathbf{2}^{2-}$ formed by addition of sodium dithionite in water, resulting in a substantial gain of luminescence intensity compared to that of non-reduced complex **2**. The detailed description of these processes requires additional studies at variable temperatures and pH, which are currently under way.

EXPERIMENTAL

Materials and Syntheses

All syntheses were performed under an inert atmosphere of dry nitrogen, using standard Schlenk techniques.

Toluene, acetonitrile and butyronitrile (all Acros) were freshly distilled from P_2O_5 , and THF (Acros) from Na/benzophenone under nitrogen.

The following compounds were prepared according to literature procedures: (i) ferrocenium tetrafluoroborate, FcBF_4 , from HBF_4 and ferrocene¹⁷, (ii) 5,6-bis(bromomethyl)-1,10-phenanthroline photochemically¹⁰ from 5,6-dimethyl-1,10-phenanthroline and *N*-bromosuccinimide (both Fluka), and (iii) $[\text{RuCl}_2(\text{bpy})_2]$ from $\text{RuCl}_3 \cdot 3\text{H}_2\text{O}$ (JM)¹⁸. The supporting electrolyte tetrabutylammonium hexafluorophosphate, Bu_4NPF_6 (Aldrich), was recrystallised twice from ethanol and dried under vacuum at 80 °C overnight. Cobaltocene, ferrocene (both Aldrich) and sodium dithionite, $\text{Na}_2\text{S}_2\text{O}_4 \cdot \text{H}_2\text{O}$ (BDH), were used as received. Aluminum oxide for column chromatography was purchased from Fluka (type 507 C neutral, Brockmann grade 1, particle size 0.05–0.15 mm, pH 7.0 ± 0.5).

Elemental analyses were conducted at the University of Applied Sciences of Western Switzerland, Fribourg.

*Anthra[2,3-*f*][1,10]phenanthroline-10,15-quinone* (**1**). 5,6-Bis(bromomethyl)-1,10-phenanthroline (0.15 g, 0.41 mmol) and 1,4-naphthoquinone (0.26 g, 1.63 mmol) were suspended in

dry toluene (250 ml) in a 500-ml round-bottom flask. The grey suspension was refluxed under argon for 12 h. During this time, the suspension colour turned orange-red and finally dark purple. After cooling to room temperature and filtration, the filtrate was divided into three fractions of equal volumes and 6 M HCl (75 ml per fraction) was added. The resulting suspension was stirred for 1 day. The purple precipitate was then filtered off, washed successively with water, toluene and diethyl ether and dried overnight under reduced pressure at 45 °C. Yield 44 mg (60 %). ^1H NMR (DMSO- d_6 , 300 MHz; see Chart 2): 8.00 (2 H, H_B); 8.10 (2 H, H_E); 8.30 (2 H, H_E); 9.23 (2 H, H_C); 9.50 (2 H, H_D); 9.64 (2 H, H_A). MS (ESI), m/z : 361 (M^+).

Due to its poor solubility in common organic solvents, crude ligand **1** was further used without purification for the synthesis of complex **2**.

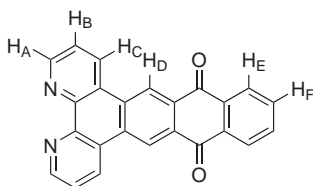


CHART 2

$[\text{Ru}(\text{bpy})_2][\text{PF}_6]_2$ (**2**). $[\text{RuCl}_2(\text{bpy})_2]$ (39 mg, 0.08 mmol) and ligand **1** (23 mg, 0.07 mmol) were suspended in ethylene glycol (10 ml) in a 50-ml round-bottom flask and heated under stirring at 150 °C for 2 h. Ethylene glycol was removed under reduced pressure and replaced by water (25 ml). Ammonium hexafluorophosphate (70 mg) was added in the next step and the suspension was stirred slowly for 1.5 h. The precipitate was isolated by suction filtration and washed with diethyl ether. The crude complex was extracted with acetone and purified on SiO_2 plates, using MeCN/MeOH/ H_2O /saturated aqueous KNO_3 (40:10:10:1, volume ratios) as the mobile phase. After drying, final purification of the orange product was accomplished by column chromatography over neutral aluminium oxide, using acetone/water (99:1) as eluent. Yield 38 mg (45%). ^1H NMR (CD_3CN , 300 MHz; see Charts 2 and 3): 7.25 (t, 2 H, H₈); 7.47 (t, 2 H, H₈); 7.67 (d, 2 H, H₇); 7.84 (m, 2 H, H_{2/7}); 7.92 (dd, 2 H, H₆); 8.05 (t, 2 H, H₉); 8.12 (t, 2 H, H₉); 8.17 (d, 2 H, H₁); 8.32 (dd, 2 H, H₅); 8.53 (t, 4 H, H_{10/10}); 9.38 (d, 2 H, H₃); 9.60 (s, 2 H, H₄). ^{13}C NMR (CD_3CN , 75 MHz): 125.33, 125.68, 128.38, 128.50, 128.81, 129.00, 131.12, 133.32, 134.39, 135.06, 136.22, 139.27, 150.23, 153.27, 153.51, 154.59, 158.29, 158.48. MS (ESI), m/z : 919 (M^+), 387 (M^{2+}). For $\text{C}_{44}\text{H}_{28}\text{F}_{12}\text{N}_6\text{O}_2\text{P}_2\text{Ru}$ (1063.7) calculated: 49.68% C, 2.65% H, 7.90% N; found: 50.28% C, 2.45% H, 6.88% N.

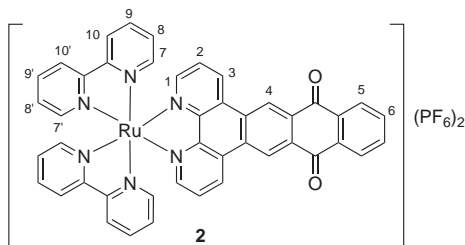


CHART 3

Physical Measurements

Spectroscopy. ESI (electron spray ionisation) mass spectra were obtained with a Bruker FTMS 4.7 T Bio APEXII spectrometer.

Electronic absorption spectra were recorded using Perkin–Elmer Lambda 18 and Hewlett–Packard 8453A diode-array spectrophotometers, and ^1H and ^{13}C NMR spectra on a Varian Gemini 300 spectrometer. The molar absorption coefficient for the MLCT band of **2** was determined for four different concentrations of the complex in the range 10^{-6} – 10^{-5} mol l^{-1} .

Continuous-wave emission spectra were measured on a Spex Fluorolog 1681 spectrofluorimeter equipped with a Xe arc light source, a Hamamatsu R928 photomultiplier tube detector and double excitation and emission monochromators. Emission spectra were corrected for source intensity and detector response using standard correction curves. Deaerated solutions were prepared by the freeze-pump-thaw technique on a high-vacuum line. Luminescence quantum yields (Φ_{em}) were measured in optically dilute solutions ($A \sim 0.1$), using standard $[\text{Ru}(\text{bpy})_3]^{2+}$ ($\Phi_{\text{em}} = 0.012$ and 0.060 in aerated and deaerated acetonitrile^{9a}, respectively), according to Eq. (1) (ref.¹⁹)

$$\Phi_{\text{em}}^{\text{s}} = \Phi_{\text{em}}^{\text{r}} (I_{\text{s}}/I_{\text{r}})(A_{\text{r}}/A_{\text{s}})(\eta_{\text{s}}/\eta_{\text{r}})^2 \quad (1)$$

where subscripts s and r denote the sample and reference, respectively. The symbol I stands for the integrated emission intensity, A is the absorbance at the excitation wavelength and η the refractive index of the solvent.

Time-resolved emission measurements were performed at single wavelength, using a continuously tunable (420–710 nm) Coherent Infinity XPO laser as excitation source. The emitted light was collected in an Oriel monochromator, detected with a Hamamatsu P28 photomultiplier tube and recorded with a Tektronix TDS3052 (500 MHz) oscilloscope. A photodiode was used as external trigger source. Optically dilute ($A < 0.3$) sample solution were used.

Nanosecond transient absorption (ns TA) spectra of deaerated solutions were obtained by irradiating the samples with 2-ns pulses of the 450 nm line (typically 4 mJ pulse⁻¹) of the Coherent Infinity XPO laser working at 10 Hz. The probe light from a low-pressure, high-power EG&G FX-504 Xe lamp was passed through the sample cell and dispersed with an Acton Spectra-Pro-150 spectrograph equipped with 150 or 600 mm⁻¹ grating and a 400 μm slit, resulting in a 6 or 1.2 nm maximum resolution, respectively. The data collection system consisted of a gated intensified CCD detector (Princeton Instruments ICCD-576EMG/RB), a programmable pulse generator (PG-200), and an EG&G Princeton Applied Research Model 9650 digital delay generator.

Electrochemistry. Cyclic and differential pulse voltammograms of 10^{-3} M samples in 10^{-1} M Bu_4NPF_6 electrolyte solution were recorded in a gas-tight, single-compartment cell equipped with a platinum disk working electrode (apparent surface area 0.42 mm²), a coiled platinum wire auxiliary electrode and a silver wire pseudoreference electrode. The cell was connected to a computer-controlled PAR Model 283 potentiostat. All electrode potentials are reported against the ferrocene/ferrocenium (Fc/Fc^+) redox couple used as an internal standard²⁰. Conversion to other reference electrode scales can be found elsewhere²¹.

Spectroelectrochemical experiments were performed with an optically transparent thin-layer electrochemical (OTTLE) cell²² equipped with a Pt minigrid working electrode (32 wires per cm) and CaF_2 windows. The potential during the thin-layer electrolyses was controlled

with a PA4 (EKOM, Czech Republic) potentiostat. The concentration of the spectroelectrochemical samples was 1×10^{-3} mol l⁻¹.

We thank the National Swiss Science Foundation for funding through the NFP 47 programme. Professor Luisa De Cola (Universität Münster) is acknowledged for valuable discussions and support of this work. Mr R. T. F. Jukes (Universiteit van Amsterdam) kindly helped with measurements of some of the emission spectra.

REFERENCES

1. Crossley M. J., Johnston L. A.: *Chem. Commun.* **2002**, 1122.
2. Wasielewski M. R.: *Chem. Rev.* **1992**, *92*, 435.
3. Yan P., Holman M. W., Robustelli P., Chowdhury A., Ishak F. I., Adams D. M.: *J. Phys. Chem. B* **2005**, *109*, 130.
4. Goudle V., Harriman A., Lehn J.-M.: *J. Chem. Soc., Dalton Trans.* **1993**, 1034.
5. McCall J., Alexander C., Richter M. M.: *Anal. Chem.* **1999**, *71*, 2523.
6. Opperman K. A., Mecklenburg S. L., Meyer T. J.: *Inorg. Chem.* **1994**, *33*, 5295.
7. Borgström M., Johansson O., Lomoth R., Berglund Baudin H., Wallin S., Sun L., Åkermark B., Hammarström L.: *Inorg. Chem.* **2003**, *42*, 5173.
8. Benniston A., Chapman G. M., Harriman A., Rostron S. A.: *Inorg. Chem.* **2005**, *44*, 4029.
9. a) Albano G., Belser P., De Cola L., Gandolfi M. T.: *Chem. Commun.* **1999**, 1171;
b) Albano G., Belser P., Daul C.: *Inorg. Chem.* **2001**, *40*, 1408; c) Batista E. R., Martin R. L.: *J. Phys. Chem. A* **2005**, *109*, 3128.
10. Barton J. W., Shepherd M. K., Willis R. J.: *J. Chem. Soc., Perkin Trans. 1* **1986**, 967.
11. Fujihara T., Okamura R., Wadu T., Tanaka K.: *Dalton Trans.* **2003**, 3221.
12. Babaei A., Connor P. A., McQuillan A. J.: *J. Chem. Educ.* **1997**, *74*, 1200.
13. Keyes T. E., Jayaweera P. M., McGarvey J. J., Vos J. G.: *J. Chem. Soc., Dalton Trans.* **1997**, 1627.
14. Krejčík M., Vlček A. A.: *J. Electroanal. Chem.* **1991**, *313*, 243.
15. Heath G. A., Yellowless L. J., Braterman P. S.: *J. Chem. Soc., Chem. Commun.* **1981**, 287.
16. Víchová J., Hartl F., Vlček A., Jr.: *J. Am. Chem. Soc.* **1992**, *114*, 10903.
17. Hendrickson D. N., Sohn Y. S., Gray H. B.: *Inorg. Chem.* **1971**, *10*, 1559.
18. Hua X: *Ph.D. Thesis*. University of Fribourg, Fribourg 1993.
19. Demas J. N., Crosby G. A.: *J. Phys. Chem.* **1971**, *75*, 991.
20. Gritzner G., Kůta J.: *Pure Appl. Chem.* **1984**, *56*, 461.
21. Pavlishchuk V. V., Addison A. W.: *Inorg. Chim. Acta* **2000**, *298*, 97.
22. Krejčík M., Daněk M., Hartl F.: *J. Electroanal. Chem. Interfacial Electrochem.* **1991**, *317*, 179.